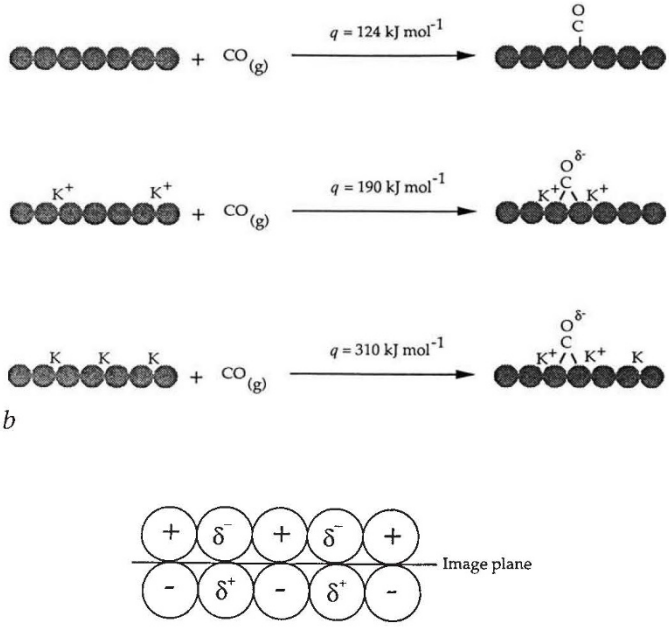

FIG. 3 *a*, Schematic of the CO interaction as θ_K is increased, and of the related heat of adsorption *q*. *b*, Image charge ionic bilayer lattice formed at high θ_K.

K^+CO^- islands within the 50-ms pulse, and we associate the heat released with the re-ionization of covalently bonded K adatoms and the associated electrostatic interaction terms. For larger precoverages of K, however, the heat release is smaller when CO is initially dosed onto the surface, as shown in Fig. 1 for $\theta_K = 0.3$ monolayers, and rises with increasing CO coverage to the same maximum value of 310 kJ mol^{-1}. At high K coverages there are relatively few unblocked sites on the surface, and this may reduce the mobility of adsorbed CO across the surface. Initially, therefore, at relatively high θ_K it may be that small $K^+CO^-K^+$ islands are formed. Only as these islands coalesce is the full Madelung energy involved, producing the observed increase in adsorption heat with coverage. At high K coverages there are, therefore, two dominant contributions to the CO adsorption heat: the increased CO $2\pi^*$ population[17], which contributes, from our low θ_K data, a 70 kJ mol^{-1} increase; and ionization of K adatoms, contributing a further ~125 kJ mol^{-1} when large islands are formed. This second component, consisting of K re-ionization and Madelung terms, is important for understanding catalytic processes as it indicates that the local environment about the CO is ionic, even at high precoverages of K. □

Received 26 June 1992; accepted 14 October 1992.

1. Mross, W. D. *Catal. Rev. Sci. Engng* **25**, 591–637 (1983).
2. Bonzel, H. P. *Surf. Sci. Rep.* **8** (1988).
3. Kiskinova, M. P. *Poisoning and Promotion in Catalysis based on Surface Science Concepts* (Elsevier, Amsterdam, 1992).
4. Heskett, D. *Surf. Sci.* **199**, 67–86 (1988).
5. Bonzel, H. P., Bradshaw, A. M. & Ertl, G. (eds) *Physics and Chemistry of Alkali Metal Adsorption* (Elsevier, Amsterdam, 1989).
6. Lackey, D. & King, D. A. *J. chem. Soc. Faraday I* **83**, 2001–2013 (1987).
7. Borroni-Bird, C. E. & King, D. A. *Rev. Sci. Instrum.* **62**, 2177–2185 (1991).
8. Borroni-Bird, C. E., Al-Sarraf, N., Andersson, S. & King, D. A. *Chem. Phys. Lett.* **183**, 516–520 (1991).
9. Tracy, J. C. *J. chem. Phys.* **56**, 2736–2747 (1972).
10. Gurney, R. W. *Phys. Rev.* **47**, 479–482 (1935).
11. Luftman, H. S., Sun, Y.-M. & White, J. M. *Appl. Surf. Sci.* **19**, 59–72 (1984).
12. Whitman, L. J. & Ho, W. *J. chem. Phys.* **90**, 6018–6025 (1989).
13. Kumar, S., Sands, W. D., Yates, J. T. & Janda, K. C. *J. Am. chem. Soc.* **113**, 3684–3688 (1991).
14. Scheffler, M. *et al. Physica* B**172**, 143–153 (1991).
15. Benesh, G. A. & King, D. A. *Chem. Phys. Lett.* **191**, 315–319 (1992).
16. Finnis, M. W. *Surf. Sci.* **241**, 61–72 (1991).
17. Nørskov, J. K., Holloway, S. & Lang, N. D. *J. Vac. Sci. Technol.* A **3**, 1668–1672 (1985); *Surf. Sci.* **137**, 65–78 (1984).
18. Gerlach, R. L. & Rhodin, T. N. *Surf. Sci.* **19**, 403–426 (1970).

ACKNOWLEDGEMENTS. We thank J. Chevallier for thin-film single crystals. The SERC (UK) is acknowledged for an equipment grant, and for a studentship to N.A.-S.; and the NSERC (Canada) is acknowledged for a fellowship to J.T.S.

Evidence for massive discharges of icebergs into the North Atlantic ocean during the last glacial period

Gerard Bond*, Hartmut Heinrich†, Wallace Broecker*, Laurent Labeyrie‡, Jerry McManus*, John Andrews§, Sylvain Huon‖, Ruediger Jantschik¶, Silke Clasen#, Christine Simet, Kathy Tedesco‡, Mieczyslawa Klas*, Georges Bonani†† & Susan Ivy**

* Lamont-Doherty Geological Observatory, Palisades, New York 10964, USA
† Bundesamt für Seeschiffahrt und Hydrographie, Postfach 30 12 20, 2000 Hamburg 36, Germany
‡ C.F.R. Laboratoire mixte CNRS-CEA, Domaine du CNRS, 91198, Gif-sur-Yvette Cedex, France
§ Institute of Arctic and Alpine Research and Geological Sciences Box 450, University of Colorado, Boulder, Colorado 80309 USA
‖ Département de Minéralogie, 13 rue des Maraichers, CH-1211 Geneve 4, Switzerland
¶ Institut de Géologie, 11, rue E. Argand, CH-2007 Neuchâtel, Switzerland
# Abteilung Sediment-Geologie, Institut für Geologie und Paläontologie, Goldschmidtstrasse 3, W-3400 Göttingen, Germany
** Institut für Geologie und Paläontologie, Sigwartstrasse 10, 7400 Tübingen, Germany
†† Institut für Mittelenergiephysik, ETH Honggerberg, CH-8093 Zurich, Switzerland

SEDIMENTS in the North Atlantic ocean contain a series of layers that are rich in ice-rafted debris and unusually poor in foraminifera[1]. Here we present evidence that the most recent six of these 'Heinrich layers', deposited between 14,000 and 70,000 years ago, record marked decreases in sea surface temperature and salinity, decreases in the flux of planktonic foraminifera to the sediments, and short-lived, massive discharges of icebergs originating in eastern Canada. The path of the icebergs, clearly marked by the presence of ice-rafted detrital carbonate, can be traced for more than 3,000 km—a remarkable distance, attesting to extreme cooling of surface waters and enormous amounts of drifting ice. The cause of these extreme events is puzzling. They may reflect repeated rapid advances of the Laurentide ice sheet, perhaps associated with reductions in air temperatures, yet temperature records from Greenland ice cores appear to exhibit only a weak corresponding signal. Moreover, the 5–10,000-yr intervals between the events are inconsistent with Milankovitch orbital periodicities, raising the question of what the ultimate cause of the postulated cooling may have been.

The most detailed study of the sediment composing the Heinrich deposits has been made on cores from DSDP site 609[2] (Fig. 1). High percentages of ice-rafted detritus (IRD) and low concentrations of foraminifera clearly define the six deposits that formed during the last glacial period (Fig. 2). Foraminiferal stratigraphy indicates that these deposits correlate directly with the six deposits originally identified by Heinrich in the Dreizack seamount area[2] (Fig. 1). We have now traced Heinrich deposits in other cores from the North Atlantic and Labrador Sea (Fig. 1), demonstrating that they are widespread features of the North Atlantic ocean. Radiocarbon measurements by

accelerator mass spectrometry (AMS) at DSDP site 609 date the first three deposits at ~14,300, ~21,000 and ~28,000 years (Table 1), and extrapolation of ^{14}C-based sedimentation rates dates the last three at ~41,000, ~52,000 and ~69,000 years (Fig. 1). Comparable AMS ages for the first three layers have been obtained from three other cores (Table 1).

One of the most unusual properties of the Heinrich deposits is the presence of prominent layers with 20% to 25% detrital limestone and dolomite, a composition markedly different from that in the ambient glacial sediment which consists mostly of quartz and feldspar, variable amounts of black volcanic glass and only a few per cent detrital carbonate (see for example Fig. 2). These distinctive layers have a well defined distribution in the northern Atlantic (Fig. 1; Table 3). In the southwest, all six Heinrich deposits contain a layer with abundant detrital carbonate. To the north and east, however, H3 and H6 lack these layers, and their IRD resembles that of the ambient sediment. Still farther to the north and in the southernmost samples, none of the Heinrich deposits identified so far contain detrital carbonate. Hence, layers rich in detrital carbonate are confined to the belt of high IRD accumulation that formed during the last glaciation[3] (Fig. 1).

Evidence of at least one source of the carbonate IRD has been found in the Labrador Sea (Fig. 1). Here, H1 and H2 contain thick layers rich in detrital carbonate (Tables 1-3) that was derived from nearby limestone and dolomite bedrock in Hudson Strait[4,5] (Fig. 1). A source in eastern Canada is further supported by the marked westward increase in thicknesses of the carbonate-rich layers (Fig. 1). In addition, in the Dreizack cores the <2-μm carbonate-free fraction in H1, 2, 4 and 5 has an average K/Ar age of 897 Myr, contrasting with average ages of 442 Myr for the >2-μm ambient glacial sediment[6,7] (Fig. 2). The older ages are evidence of detrital clay with large amounts of Precambrian material[6,7], ample sources of which occur in eastern Canada.

Two other features of the Heinrich deposits are worthy of mention. First, each layer rich in detrital carbonate accumulated rapidly. This is indicated by their sharp bases as revealed in X-radiographs of Dreizack[8,9] and DSDP site 609 cores, and by increased fluxes of lithic grains comprising the carbonate IRD in H1 and H2 (Table 2). Foraminifera are well preserved in these layers and our flux estimates are not affected by dissolution. Second, all six Heinrich deposits contain evidence of surface water with extremely low temperature, low flux of planktonic foraminifera and low salinity. In each deposit, the planktonic species *Neogloboquadrina pachyderma* (left-coiled) dominates the foraminifera population (Fig. 2), indicating deep southward penetration of polar water. In DSDP site 609, the flux of planktonic foraminifera of size >150 μm dropped markedly during

TABLE 1 AMS radiocarbon dates for DSDP 609, HU75-55, V23-81 and V23-16

Core		Depth (cm)		Corrected age* (years)	Error (years)
DSDP 609 (*G.b.*)		63-65		11,980†	120
SDSP 609		64-66		11,180‡	190
DSDP 609		69-70		11,020‡	190
DSDP 609		73-75		12,350‡	220
DSDP 609		**75-77**		**13,490‡**	**220**
DSDP 609 (*G.b.*)	**H1**	**79-81**	← *Hc*	**13,250‡**	**090**
DSDP 609		**84-85**		**14,590‡**	**230**
DSDP 609		87-88		15,960‡	240
DSDP 609		90-91		16,360‡	150
DSDP 609		98-99		16,960‡	120
DSDP 609		105-107		18,940‡	220
DSDP 609		**110-111**		**19,970‡**	**330**
DSDP 609	**H2**	**111-112**		**20,550§**	**260**
DSDP 609		**112-113**	*Hc*	**21,110‡**	**220**
DSDP 609		**115-116**		**21,370‡**	**220**
DSDP 609		118-120		22,380‡	340
DSDP 609 (*G.i.*)		139-141		25,260‡	440
DSDP 609		**143-144**		**26,570‡**	**490**
DSDP 609	**H3**	**147-149**		**26,170‡**	**310**
DSDP 609		**153-155**		**29,170†**	**660**
DSDP 609		166-167		30,080‡	680
DSDP 609 (*G.i.*)		174-176		30,720†	730
HU75-55	H1→	81		13,235	190
HU75-55		116		14,610	105
HU75-55	H2→	181		19,455	210
HU75-55		250		21,105	240
V23-81		198-199		12,320§	220
V23-81	H_1→	215-216		13,260§	210
V23-81		249-250		16,550‡	190
V23-81	H_2→	264-265		18,530‡	240
V23-81		335-336		21,950‡	310
V23-81	H_3→	340-341		23,090‡	370
V23-81		400-401		31,250‡	690
V23-81		418-419		30,150‡	770
V23-16	H1→	29-30		10,050‡	150
V23-16		54-55		15,370‡	220
V23-16	H2→	62-63		16,670‡	280
V23-16		144-145		23,400‡	390
V23-16	H3→	184-185		28,240‡	600
V23-16		207-208		31,230‡	880

* Corrected for assumed 400-yr difference between surface water carbon and atmospheric carbon. *G.b.* indicates analyses done on *G. bulloides*, *G.i.* indicates analyses done on *G. inflata*. All other measurements are on *N. pachyderma* (l.c.) H1 and so on are Heinrich deposits as defined by low foram concentrations (see for example Fig. 2). *Hc* refers to layers within Heinrich deposits that are rich in detrital carbonate IRD.

† Ref. 29.

‡ From analyses done in Zurich for this paper.

§ Ref. 19.

TABLE 2 Foraminifera and IRD sand flux estimates for DSDP 609

	Depth interval (cm)	Radiocarbon time interval	Flux of foraminifera >150 μm (number $cm^{-2}\,yr^{-1}$)	Flux of IRD >150 μm (number $cm^{-2}\,yr^{-1}$)
	64-74	1,270	29.31	3.78
	74-76	**1,140**	**5.39**	**2.58**
H1	**76-84**	**1,100**	**7.40**	***Hc*→10.50**
	84-87	**1,370**	**6.34**	**3.14**
	87-90	400	27.57	11.49
	90-105	2,580	26.87	6.07
	105-110	**1,030**	**9.89**	**4.78**
H2	**110-112**	**1,140**	**4.45**	**2.85**
	112-115	**260**	**8.53**	***Hc*→20.15**
	115-118	**1,010**	**9.78**	**5.25**
	118-139	2,880	17.24	4.17
	139-143	**1,310**	**5.58**	**1.05**
H3	**143-153**	**2,600**	**1.97**	**2.13**
	153-166	910	17.79	9.10
	166-174	540	22.76	7.02

Flux estimates were calculated using measured dry sample weights, grain and foram counts, radiocarbon age intervals and dry bulk density. Dry bulk density was calculated using wet bulk density and sediment porosity in ref. 20. Two equations were solved: flux = SI $[\sum(pc)\times\rho_{dd}]/\Delta t$, and $\rho_{dd} = \rho_{wd} - (\phi_s \times \rho_w)$, where SI is sampling interval, pc is particle count per gram. ρ_{dd} = dry bulk density, ρ_{wd} = wet bulk density, ϕ_s is sediment porosity, ρ_w is density of sea water, and Δt is time interval based on radiocarbon dates. Because layers with carbonate IRD have higher densities than ambient sediment and they lack foraminifera, the IRD flux values for those layers are a minimum. The decrease in foraminifera flux in the H layers is too large to be an artefact of variations in density and porosity of typical glacial sediment[17].

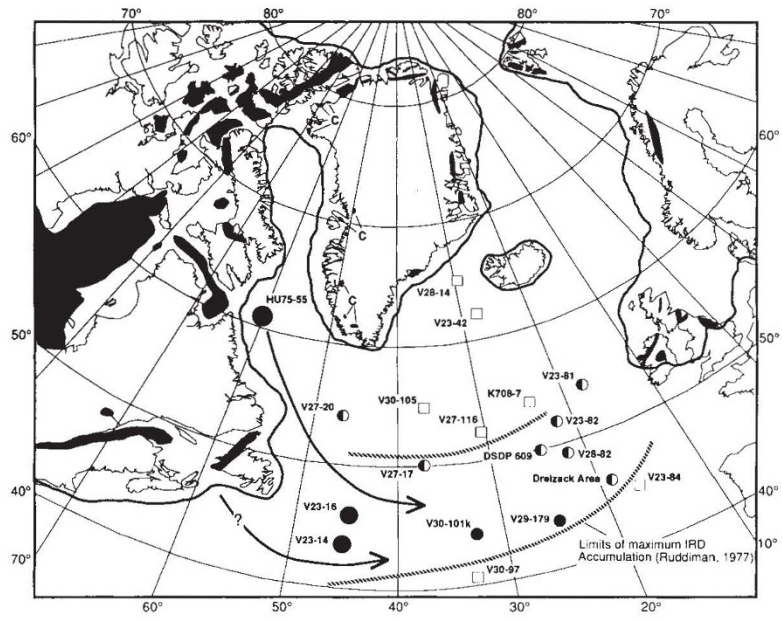

FIG. 1 Location of cores containing Heinrich deposits (deposits with unusually large concentrations of IRD and low amounts of foraminifera) and IRD unusually rich in limestone and dolomite grains. Filled circles indicate that carbonate-rich IRD is present in all Heinrich deposits identified; half-filled circles indicate that carbonate-rich IRD is absent in some of the Heinrich deposits identified; open squares indicate that carbonate-rich IRD is absent in all of the Heinrich layers identified (see Table 3). The solid black pattern is the distribution of limestone and dolomite bedrock (including submerged rocks in Hudson Bay and Hudson Strait) and the thick solid line is the approximate maximum limit of ice sheets during the last glaciation. Cs are small exposures of carbonate rocks. The westward increase in thicknesses of layers rich in carbonate IRD, indicated by increase in the size of the circles, and the widespread occurrence of limestone and dolomite in eastern Canada and northwestern Greenland are evidence that the carbonate-bearing icebergs originated in the Labrador Sea and Scotian Shelf regions. Their transit completely across the Atlantic was made possible by extreme cooling of surface waters, as indicated by the high percentages of the polar planktonic foraminifera *N. pachyderma* in the Heinrich layers (Fig. 2). The arrows show possible paths of iceberg transport.

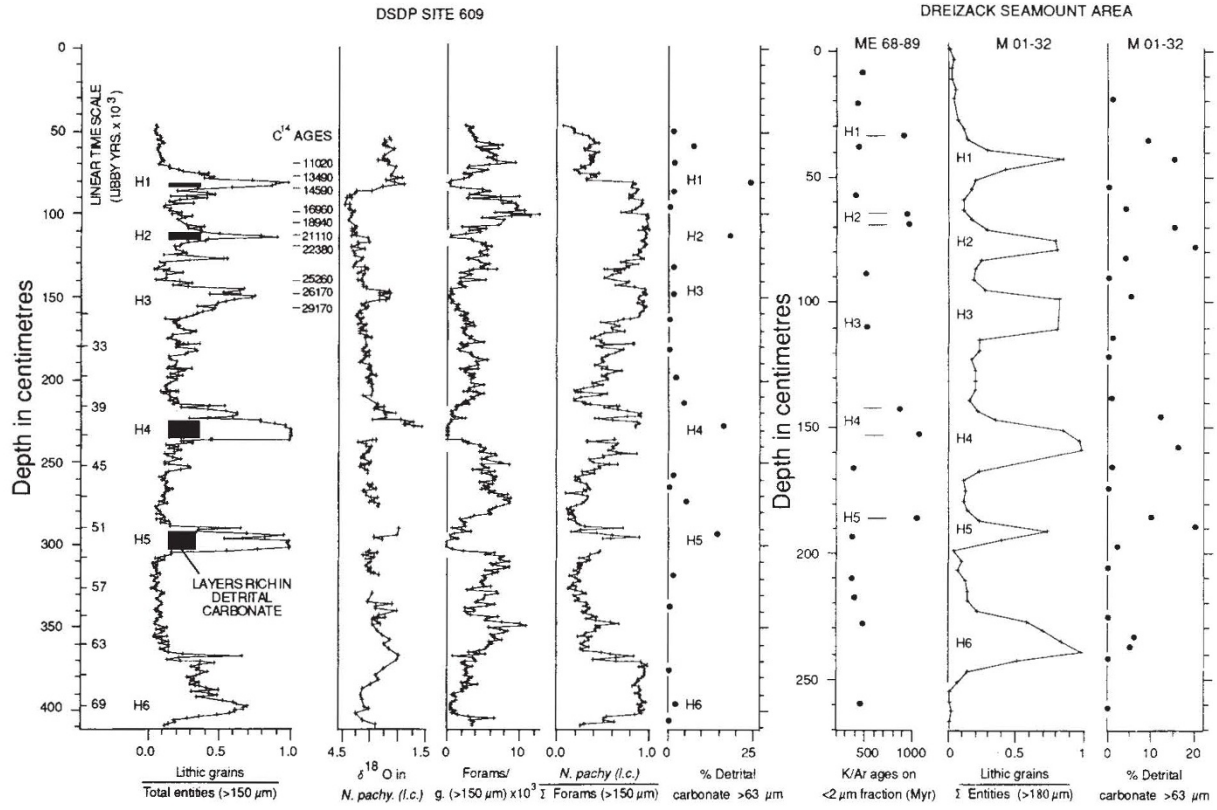

FIG. 2 Summary of radiometric, planktonic $\delta^{18}O$, foraminiferal and lithic measurements in cores from DSDP site 609 and from the Dreizack seamount area. The number of foraminifera size >150 μm per gram and the ratio of lithic grains to total entities >150 μm in cores from both localities defines the six deposits originally identified by Heinrich[1]. Microscopic examination indicates that low foraminiferal concentrations also occur in material <150 μm in the Heinrich layers. AMS C^{14} ages are from Table 1. The linear timescale begins at 175 cm (30,720 C^{14} years, Table 1), and is based on a mean sedimentation rate of 6 cm per 1,000 years given by C^{14} dating and by orbital tuning[27]. K/Ar ages from core Me 68–89 are from refs 6 and 7. The $\delta^{18}O$ measurements were made at Gif-sur-Yvette. ($\delta^{18}O = (^{18}O/^{16}O)_{sample}/(^{18}O/^{16}O)_{standard} - 1$, where standard is PDB.) The gaps in the ratio of *N. pachyderma* to total of foraminifera and in the $\delta^{18}O$ record in DSDP site 609 are intervals where the number of foraminifera is nearly zero. In these cores, four of the Heinrich deposits (H1, 2, 4 and 5) contain layers with unusually high percentages of carbonate IRD that was derived from sources in eastern Canada (Fig. 1). The black bars in DSDP 609 are the positions of these layers in the core as defined by their distinctive appearance in X-radiographs. The detrital carbonate constitutes 20% to 25% of the IRD in both the Dreizack area and at DSDP site 609, determined by line counting the >63 μm fraction with a petrographic microscope. Based on visual estimates of DSDP site 609 material, detrital carbonate consitutes 40% to 60% of the <63 μm fraction. The detrital carbonate grains are rounded to subrounded and have fine-grained recrystallized textures. At one locality in the Dreizack area, core 244, oolites and fragments of echinodems have been identified in the carbonate IRD. In addition, the layers rich in detrital carbonate have small amounts of fine-grained authigenic dolomite and unusually low porosities that average about one half that of typical deep sea muds (refs 8,9). The clay mineralogy of layers H1, 2, 4 and 5 in the Mount Dreizack cores also is unusual, consisting of abundant material from freshly derived acidic and metamorphic rocks and lacking the smectitic products of weathered basalts found in the ambient sediment (refs 6, 28).

TABLE 3 Thicknesses of detrital carbonate-rich layers within Heinrich deposits (H)

Core	Latitude (N)	Longitude (W)	Water depth (m)	H1		H2		H3		H4		H5		H6	
				d	*t*	*d*	*t*	*d*	*t*	*d*	*t*	*d*	*t*	*d*	*t*
HU75-55	61° 30′	58° 39′	2,500	90	40	210	69	*	*	*	*	*	*	*	*
V23-16	46° 00′	45° 03′	2,813	45	25	120	35	205	20	270	50	375	8	550	12
V23-14	43° 24′	45° 15′	3,177	*	*	55	10	120	20	150	15	265	25	380	15
V28-82	49° 27′	22° 16′	3,935	60	5	98	15		*	192	23	*	*	*	*
V30-101k	44° 06′	32° 30′	3,504	37	3	52	8	80	5	98	4	*	*	*	*
DSDP 609	49° 53′	24° 14′	3,884	82	1	113	5	150	0	229	10	296	10	400	0
V29-179	44° 01′	24° 32′	3,331	60	2	83	3	120	1	200	4	*	*	*	*
Mo1-32	47° 35′	28° 56′	4,070	42	3	78	7	105	0	157	12	192	5	236	0
V23-82	52° 35′	21° 56′	3,974	90	1	152	5	190	0	270	4	340	2	440	0
V23-81	54° 15′	16° 50′	2,393	220	1	329	3	383	0	495	3	584	2	760	0
V30-105	54° 31′	36° 30′	2,758	110	0	*	*	*	*	*	*	*	*	*	*
V27-17	50° 05′	37° 18′	4,054	33	0	49	5	70	2	95	3	*	*	147	2
V27-20	54° 00′	46° 12′	3,510	56	0	96	2	125	0	210	8	*	*	*	*
V27-116	52° 50′	30° 20′	3,202	43	0	65	0	*	*	*	*	*	*	*	*
V28-14	64° 47′	29° 34′	1,855	150	0	*	*	*	*	*	*	*	*	*	*
V23-42	62° 11′	27° 56′	1,514		NH	*	*	*	*	*	*	*	*	*	*
K708-7	53° 56′	24° 05′	3,502	40	0	100	0		NH		NH		NH	200	0
V30-97	41° 00′	32° 56′	3,371	70	0	*	*	*		*	*	*	*	*	*
V23-82	46° 00′	16° 55′	4,513	50	0	*	*	100	*	*	*	*	*	*	

Core locations are given in Fig. 1. Thicknesses (*t*) and depths (*d*) are in centimetres; where layer rich in detrital carbonate is present, depths are at the approximate middle of that layer; otherwise depths are at the middle of the low foraminiferal zone. NH–No Heinrich deposit (that is, no deposit with low abundance of foraminifera) at expected depth. Data for identification and correlation of Heinrich deposits as follows: HU75-55, DSDP 609 (Table 1, refs 2, 4, 5); M01-32 (ref. 1); V23-81 (refs 19, 21 and W. F. Ruddiman, unpublished data from the National Geophysical Data Center (NOAA); K708-7 (refs 21–23, and W. F. Ruddiman, NOAA unpublished data); V28-82 (% *N. pachyderma* from G.B. *et al.*, manuscript in preparation); V28-14 (refs 21, 23, 24); V23-16, V23-82, V23-83, V30-101k, V29-179, V30-105, V27-17, V27-20, V27-116, V23-42, V30-97 (refs 21, 23, 25, 26 and W. F. Ruddiman, NOAA unpublished data; and % *N. pachyderma* from G.B. *et al.*, manuscript in preparation). In V23-84 foraminiferal abundances have not been measured, but low coccolith zones occur at probable depths of H1 and H3 (ref. 26) and are taken as evidence of Heinrich deposits.

* No data available.

formation of at least the first three deposits (Table 2). This implies a reduction in the number of foraminifera living in the surface water, although we note that dissolution of foraminifera has occurred in H3. A reduction in the number of foraminifera in surface water could be associated with changes in primary productivity, but it could also reflect other changes in surface water, associated directly with temperature or salinity. Conspicuous decreases in planktonic $\delta^{18}O$ also occur in all six of the Heinrich deposits (Fig. 2). As the foraminiferal assemblages dictate cold conditions, sea surface salinities must have dropped markedly during deposition of each layer.

The evidence we have so far allows us to propose a tentative explanation for Heinrich layers and their unusual mineralogy. First, we note that the layers with abundant detrital carbonate lie within but do not extend through the Heinrich deposits (Fig. 2). This leads us to view Heinrich deposits as a composite of two processes. One was a drop in sea surface temperatures accompanied by reduction of the flux of planktonic foraminifera, accounting in part for the high lithic to foraminifera ratios originally noted by Heinrich[1]. The other, indicated by rapid deposition of the carbonate-rich IRD, was a brief but massive discharge of icebergs, occurring within but not spanning the interval of low surface temperatures. The rapid deposition of this IRD overwhelmed the already reduced flux of foraminifera, producing layers within the Heinrich deposits nearly devoid of foraminifera (Fig. 2). We suggest that shortly after surface temperatures and foraminifera flux began to drop, ice streams in eastern Canada (and possibly in northwestern Greenland) began to advance rapidly, leading to massive calving as ice fronts reached maximum seaward positions. This led to the release of large amounts of glacier ice, much of it carbonate-bearing, into the Labrador Sea and perhaps into the Scotian shelf as well. Cold sea surface temperatures slowed melting and the icebergs drifted into the North Atlantic. Rapid transit of huge amounts of this ice eastward along the southern edge of the polar gyre led to rapid deposition of carbonate-rich IRD in a wide belt, reaching completely across the ocean during four of the events.

The absence of the carbonate-rich layers south of the IRD belt (Fig. 1) probably reflects complete melting of ice upon reaching warm water south of the glacial polar front[3]. Similarly, the absence of carbonate-rich IRD in H3 and H6 in cores within the belt is probably a consequence of warmer sea surface temperature causing melting of the ice before it could traverse the width of the Atlantic. The absence of the carbonate-rich IRD in virtually all of the Heinrich deposits identified farther north is consistent with the glacial circulation pattern in which discharge of ice from the Labrador Sea was carried southwards and then in a broad arc northeastwards along the southern boundary of the polar gyre[10].

Melting of the huge quantities of ice drifting across the North Atlantic must have been an important factor in the sudden lowering of surface salinities implied by the $\delta^{18}O$ measurements[1]. Assuming a $\delta^{18}O$ of −35‰ for glacial ice[11] and ignoring the decrease in temperature implied by the foraminiferal speciation, the ~1‰ $\delta^{18}O$ changes require mixing only about 1 part iceberg meltwater with about 30 parts sea water. We note that the accompanying salinity drop is probably enough to shut down the North Atlantic's thermohaline circulation.

Perhaps the most important result of our study is its evidence of repeated, rapid advances of ice sheets in eastern North America and the questions it raises about the cause of those events. One explanation is stochastic surging[2], but that does not account for evidence of extreme cooling of surface water and reduced flux of planktonic foraminifera before and after the discharge of ice into the ocean. The same evidence makes it unlikely that the discharges of ice and melt products were the sole cause of the lowered sea surface temperatures. If atmospheric cooling accompanied the shift of polar water southward, the ice advances may have been forced by falling temperatures. The time intervals between the successive Heinrich layers, however, are shorter than orbital precession cycles (19 and 23 kyr), raising the question of what would have caused the atmospheric cooling. So far, only H1 and H2 have been linked directly to advances of ice streams, and only in the limited area of Hudson Strait[4,5]. Our study raises questions of whether other parts of the Laurentide ice sheet discharged carbonate-bearing icebergs at the same times, whether there are glacial records of the older Heinrich events in eastern North America, and whether there were correlative advances of the Greenland, Fennoscandian and Barents Sea ice sheets[12–18]. If so, those will be the first indications that large portions of Northern Hemisphere ice

sheets advanced synchronously on timescales less than those of the Milankovitch cycles, events that are not incorporated in current models of ice-sheet dynamics. □

Received 8 May; accepted 8 October 1992.

1. Heinrich, H. *Quat. Res.* **29,** 142–152 (1988).
2. Broecker, W. S., Bond, G., Klas, M., Clark, E. & McManus, J. *Clim. Dynam.* **6,** 265–273 (1992).
3. Ruddiman, W. *Geol. Soc. Am. Bull.* **88,** 1813–1827 (1977).
4. Andrews, J. T. & Tedesco, K. *Geology* (in the press).
5. Tedesco, K. & Andrews, J. T. *Eos* 72(44), 271 (1992).
6. Jantschik, R. & Huon, S. *Ecol. Geol. Helv.* **85,** 195–212 (1992).
7. Huon, S., Jantschik, R., Kubler, B. & Fontignie, D. *Bull. Suisse Miner. Petrogr.* **21,** 275–280 (1991).
8. Jantschik, R. & Lohoff, R. thesis Univ. of Göttingen (1987).
9. Clausen, S., Jantschik, R. & Meischner, D. *Nachr. Dt. Geol. Ges.* **43,** 121 (1990).
10. Ruddiman, W. F. & McIntyre, A. *Science* **212,** 617–627 (1981).
11. Dansgaard, W. *et al. Science* **218,** 1273–1277 (1982).
12. Henrich, R., Kassens, H., Vogelsang, E. & Thiede, J. *Mar. Geol.* **86,** 283–319 (1989).
13. Wolf, T. C. W. *Geomar. Rep.* **5,** 92 (1991).
14. Henrich, R. in *Init. Rep. DSDP* 104 (eds Eldholm, O. Thiede, J. & Taylor, E.) 189–232 (U.S. Govt. Printing Office, Washington, DC, 1989).
15. Vogelsang, E. *Ber. Sonderforschungsber.* **313(32),** 136 (1990).
16. Bischof, J. *Ber. Sonderforschungsber.* **313(30),** 127 (1991).
17. Kassens, H. *Ber. Sonderforschungsber.* **313(24),** 115 (1990).
18. Birgisdóttir, L. *Ber. Sonderforschungsber.* **313(34),** 112 (1991).
19. Broecker, W. S. *et al. Paleoceanography* **3,** 1–19 (1988).
20. Ruddiman, W. F. *et al. Init. Rep. DSDP* **94,** 247–349 (U.S. Govt Printing Office, Washington DC, 1987).
21. Ruddiman, W. F. & McIntyre, A. *Palaeogeogr. Palaeoclimatol. Palaeoecol.* **35,** 145–214 (1981).
22. Ruddiman, W. F., Sancetta, C. D. & McIntyre, A. *Phil. Trans. R. Soc. Lond.* B**280,** 119–142 (1977).
23. Ruddiman, W. F., McIntyre, A., Niebler-Hunt, V. & Durazzi, J. T. *Quat. Res.* **13,** 33–64 (1980).
24. Kellogg, T. B. in *Climate Changes on a Yearly to Millennial Basis* (eds Mörner, N. A. & Karlén) 123–133 (Reidel, Dordrecht, 1989).
25. Sancetta, C., Imbire, K. J., Kipp, N. G., McIntyre, A. & Ruddiman, W. F. *Quat. Res.* **2,** 363–367 (1972).
26. McIntyre, A., Ruddiman, W. F. & Jantzen, R. *Deep-Sea Res.* **19,** 61–77 (1972).
27. Ruddiman, W. F., Raymo, M. E., Martinson, D. G., Clement, B. M. & Backman, J. *Paleoceanography* **4,** 353–412 (1989).
28. Grousset, F. & Chesselet, R. *Earth planet. Sci. Lett.* **78,** 271–287 (1986).
29. Broecher, W. S., Bond, G., Klas, M., Bonani, G. & Wolfli, W. *Paleoceanography* **5,** 469–477 (1990).

ACKNOWLEDGEMENTS. We thank D. MacAyeal and G. Denton for comments on the manuscript, and J. Thiede and T. Wolf for information on possible Heinrich events in the Norwegian Sea. This research was supported in part by the NSF and NOAA. Work on the Dreizack cores was supported by a DFG grant. The planktic $\delta^{18}O$ have been measured with the support of the French CNRS, CEA and CEE(EPOCH). We thank the Ocean Drilling Program for permission to sample cores from DSDP site 609. Support for the core collection of Lamont-Doherty Geololgical Observatory is provided by the NSF and the office of Naval Research.

Primary production in the glacial North Atlantic and North Pacific oceans

Constance Sancetta

Lamont–Doherty Geological Observatory of Columbia University, Palisades, New York 10964, USA

THE conditions controlling primary production are very different in the modern North Atlantic and North Pacific oceans[1], a difference that is reflected in the composition of diatom fossils in surface sediments. By contrast, I report here evidence that during the last glacial interval the diatom assemblage, and by extrapolation the primary production, was very similar in the two regions. The modern analogues of these assemblages occur in sediments of Baffin Bay and the Sea of Okhotsk, both highly productive seas where ice is present. I infer that during the last glacial interval plankton biomass was at least as high as it is today in the North Atlantic, and was as much as an order of magnitude higher in the North Pacific. The glacial assemblage occurs in lithologies dominated by ice-rafted detritus, which is generally believed to indicate the presence of icebergs[2–6]. I hypothesize that the presence of numerous icebergs, possibly associated with sea ice, supported high production by physical mechanisms (such as turbulent mixing and enhanced density stratification) and/or biogeochemical ones (such as supply of major or trace nutrients).

In the modern world, primary production in the Pacific Ocean between 45° N and 60° N is dominated by production of picoplankton and is not limited by the availability of major nutrients. It has been suggested that picoplankton abundance is limited by efficient microzooplankton grazing, and that diatom production may be limited by very low availability of a trace element such as iron[1,7–9]. Coastal zone colour scanner (CZCS) imagery indicates a biomass of 0.3–0.5 mg C m^{-3} (ref. 10) and chlorophyll *a* concentrations rarely exceed 0.4 mg m^{-3} (ref. 9). The sediment diatom assemblage is dominated (60–80%) by *Denticulopsis seminae*[11], an endemic taxon which also dominates the diatom plankton assemblage[12].

In contrast, primary production in the same latitudes of the North Atlantic is characterized by a large spring bloom triggered by thermal stratification[1] and possibly seeded by transport from the coastal zone (R. Sambrotto, personal communication); summer production is nutrient-limited and may depend on recycled nutrients[1]. Biomass estimated from CZCS is 1.0–10.0 mg C m^{-3} (ref. 10), at least an order of magnitude higher than that in the North Pacific, and chlorophyll *a* levels during blooms exceed 1 mg m^{-3} (ref. 1). Sediments underlying this area contain abundant spores of the genus *Chaetoceros* (40–60%) and a variety of sub-tropical taxa[13]. *Chaetoceros* are characteristic of the regional spring bloom (ref. 1 and A. Weeks and R. Williams, personal communication), whereas the sub-tropical taxa probably reflect transport by the West Wind Drift[13]. The difference in sediment diatom assemblages thus parallels the modern differences in seasonal conditions of primary production.

I have examined the diatom fossil assemblage in core records spanning the last 20,000 years using two cores from the North Pacific and one from the North Atlantic. Ocean Drilling Project Site 609 is located in the central North Atlantic Ocean (49°53′ N, 24°14′ W), and recently has been the focus of studies[4,5] addressing the short intervals of massive ice-rafting (which created the so-called Heinrich deposits) during the last glacial period. I examined samples dating from about 9,000 to 23,000 yr BP, at intervals of 1,100 to 1,500 years (ages from accelerator mass spectrometry (AMS) ^{14}C dating of planktonic forminifera[4]). Samples from Heinrich zones were examined but not included in the quantitative analysis. Diatoms are extremely rare in these intervals, and it would be necessary to process large volumes of material to obtain sufficient numbers for statistically reliable results. Two cores from the North Pacific were examined at intervals of less than 1,000 years, covering the same period of time. Age control on these cores (PAR87a-02, 54°17′ N, 149°36′ W and RNDB-PC11, 51°4′ N, 167°58′ E) is based on correlation to nearby cores dated by AMS ^{14}C analysis of planktonic foraminifera[14,15].

The taxonomic difference between the two oceans persists in samples younger than 15,000 yr BP, representing the Holocene and latest glacial interval. This suggests that, throughout that time, conditions of production in the two oceans were similar to those at present. In contrast, samples representing the full glacial interval are very similar in both oceans, with the diatom assemblage characterized by *Actinocyclus curvatulus* and *Thalassiosira latimarginata*. Samples from the Pacific cores are dominated by *T. latimarginata* (40–60%), with *A. curvatulus* as a secondary component (10–20%), whereas in the Atlantic core the two taxa are present in similar proportions (15–30%). *Chaetoceros* spores are also common in the Atlantic material (30–50%), implying persistences of the spring bloom.

Modern analogues of the assemblages can be found in the western marginal seas of the two oceans. Cluster analysis shows that the assemblage in the Pacific cores is most similar ($r > 0.78$) to modern core-top assemblages in the Sea of Okhotsk[11]. The Atlantic assemblage of Site 609 seems to be similar to those reported for core-top material from Baffin Bay[16]. The latter are described as having abundant *Chaetoceros* spores (30–70%) and an average of 21% *A. curvatulus* and 13% *T. latimarginata*, values close to those observed in glacial samples from Site 609.

In modern Baffin Bay, biomass (estimated by CZCS) is about 1.0 mg C m^{-3} (ref. 10), and the average chlorophyll *a* concentration in spring is 1.7 mg m^{-3} (ref. 17). These values are within the range of those for the modern North Atlantic, from which